Producing cold from heat with aluminum carboxylate-based metal-organic frameworks

Effrosyni Gkaniatsou, Chaoben Chen, Frédéric S Cui, Xiaowei Zhu, Paul Sapin, Farid Nouar, Cedric Boissiere, Christos N Markides, Jan Hensen, Christian Serre

Article

Producing cold from heat with aluminum carboxylate-based metal-organic frameworks

Thermally driven cooling technology is an alternative solution to electric heat pumps in removing hazardous refrigerants and harnessing renewables and waste heat. Gkaniatsou et al. report a proof-of-concept full-scale adsorption chiller using MOFs as sorbents with optimized configurations derived from various characterization techniques.

Effrosyni Gkaniatsou, Chaoben Chen, Frédéric S. Cui, ..., Christos N. Markides, Jan Hensen, Christian Serre

f.s.cui@tue.nl (F.S.C.)
christian.serre@espci.psl.eu (C.S.)

Highlights

A full-scale Al-MOF based adsorption chiller is constructed

Green upscale synthesis of advanced sorbents is key to cost-effective sorption cooling

Cooling performances of MIL-160(Al) are comparable with LiBr-based absorption chiller

Solar thermal-driven adsorption chiller is a weather resilient cooling solution

Article

Producing cold from heat with aluminum carboxylate-based metal-organic frameworks

Effrosyni Gkaniatsou,[1,7] Chaoben Chen,[2,7] Frédéric S. Cui,[2,3,8,*] Xiaowei Zhu,[4] Paul Sapin,[5] Farid Nouar,[1] Cédric Boissière,[6] Christos N. Markides,[5] Jan Hensen,[3] and Christian Serre[1,*]

SUMMARY

Worldwide cooling energy demands will increase by four times by 2050. Thermally driven cooling technology is an alternative solution to electric heat pumps in removing hazardous refrigerants and harnessing renewables and waste heat. We highlight the advantages of water-stable microporous aluminum-carboxylate-based metal-organic frameworks, or Al-MOFs, as sorbents in the application of producing cold from heat. Here, we synthesize the Al-MOFs with green and scalable processes, which are prerequisites for exploring various industrial and civil applications. A proof-of-concept full-scale adsorption chiller with different Al-MOFs is built up with optimized configurations derived from various characterization techniques. The tested Al-MOFs achieve thermal efficiency above 0.6 and specific cooling power over 1 kW/kg in typical cooling scenarios. Notably, when solar thermal energy is used as the heat source in an outdoor validation, Al-MOFs are weather-resilient solutions that exhibit a stable energy conversion efficiency under fluctuating operating conditions (ambient temperature and solar irradiation).

INTRODUCTION

Cooling needs are increasing in our modern society. France, for instance, endured an unprecedented hot summer in 2019, with average temperatures of 3°C above and an anomaly peaking at 10°C relative to the last 4 decades.[1] For the entire summer, the government implemented the "Plan Canicule," a series of measures to mobilize public resources fighting against the heatwave for its many hazards regarding morbidity, mortality, and economic activities.[2,3] Although it is historical, this heat record may not remain unbroken, and in a few years. During summer 2021, the northwestern United States suffered from an exceptional heat dome associated with near-50°C record temperatures.

Most passive cooling methods that the inhabitants of Europe are accustomed to are no longer efficacious to provide proper comfort or even reduce heat exposure under harsher climate conditions; for instance, temperature difference and wind effect, the main drivers of natural ventilation, both will be weakened under these circumstances.[4] The fast growth of the mechanic cooling market is inevitable, along with the probable tremendous increase of world cooling energy consumption for buildings from 1.25 PWh in 2010 to 6.8 PWh forecasted for 2050.[5] Conventional vapor compression refrigeration systems, however, are themselves a contributing factor to the warming and anthropogenically induced hot extremes by using refrigerants with a high global warming potential and locally converting electricity into thermal

[1]Institut des Matériaux Poreux de Paris (IMAP), ESPCI Paris, Ecole Normale Supérieure, PSL University, CNRS, Paris, France

[2]Elektron Gri, 10 Rue des Trois Portes, 75005 Paris, France

[3]Department of the Built Environment, Eindhoven University of Technology, PO Box 513, 5600 MB Eindhoven, the Netherlands

[4]Department of Mechanical Engineering, Eindhoven University of Technology, PO Box 513, 5600 MB Eindhoven, the Netherlands

[5]Clean Energy Processes (CEP) Laboratory, Department of Chemical Engineering, Imperial College London, London SW7 2AZ, UK

[6]Sorbonne Université, UPMC Univ Paris 06, CNRS, UMR 7475, Chimie de la Matière de la Condensée, 75005 Paris, France

[7]These authors contributed equally

[8]Lead contact

*Correspondence: f.s.cui@tue.nl (F.S.C.), christian.serre@espci.psl.eu (C.S.)

https://doi.org/10.1016/j.xcrp.2021.100730

energy.[6,7] Achieving the climate target in the Paris Agreement requires present cooling technologies to undergo a radical paradigm shift in terms of energy efficiency and energy sources beyond the regulation on the set point temperatures.[8,9] Thermally driven chillers are a solution to counterbalancing the hazardous leak and intensive energy loads of compression cooling, among which sorption chillers using water as a working fluid exhibit the potential of reducing emissions and harnessing low-grade heat sources.[10] An exceptional advantage of sorption cooling is that the efficiency does not drop as quickly as compression cooling in high-temperature environments. Nevertheless, commercially available sorbents (e.g., hydroscopic salts, silica, zeolites), which are benchmark host materials to capture water vapor, suffer from several apparent drawbacks, including toxicity and corrosion (LiBr), inapt linear sorption isotherm curve (silica gel), costly synthesis (SAPO-34), and oversizing.[11–14]

Optimal sorbents should be non-corrosive and of reasonable cost. They should also possess high energy exchange rates, and narrow operation windows of temperature difference in the switch between adsorption and regeneration cycles. The emerging class of porous hybrid adsorbents, metal-organic frameworks (MOFs), provides technical feasibility to address the above requirements.[15] MOFs are assembled by variable metal clusters and organic linkers, giving rise to myriads of topologies with tunable pore size/shape and compositions. This is associated with hydrophilicity and water-uptake capacity that can be facilely adjusted to fit working conditions in different weather and cooling applications.[16–18] Recent advances rely mostly on high-valence metal cations (e.g., Fe^{3+}, Al^{3+}, Cr^{3+}, Ti^{4+}, Zr^{4+}) and polycarboxylates due to their attractive hydrothermal stability.[19–25] Two relevant examples are the mesoporous solids ($20 \leq \varnothing \leq 500$ Å) MIL-100 (MIL: materials from Institut Lavoisier) and MIL-101, the capillary condensation of water molecules inside the mesoporous cages of which is the major mechanism of water cluster interaction, and therefore, the sorption heat is very close to the condensing enthalpy.[19,26] Selecting these MOFs conveys the prevalent idea that the more water the pore structure can contain, the higher energy density it should be handed over. However, the latest findings lie in contrast to the assumption that a high coefficient of performance (COP) for each operation cycle of these MOFs leads to more effective energy conversion in sorption cooling.[27] In fact, the large pores create inflection points of isotherms at such high relative pressures (0.4–0.5 p/p_0) that the connected evaporator cannot maintain a relatively low temperature, failing to offset heat exchange losses. This mismatch in methodology originates mainly from the lack of synergy between materials science and thermal engineering communities, indicating that improvement in thermodynamic properties alone is insufficient.

The specific cooling power (SCP) is an equally critical figure-of-merit of a MOF chiller and it depends principally on improving the adsorption dynamics, referring to the optimization not only on the microstructure level but also of the macroscopic shaping process. The latter is often a cumbersome and time-consuming process but indispensable to pave the way to a higher technique-readiness level.[28] Only a few researchers have investigated power performance in realistic conditions. Henninger et al.[29,30] conducted thermogravimetrical measurements on the key component—a heat exchanger coated with aluminum MOFs as sorbents, which displayed rapid kinetics in response to typical temperature requirements for space cooling. Most of the extant literature tends to use small-scale heat exchangers for dynamic tests to quickly screen available adsorbents.[27,31,32]

An analysis based on calibration at reduced size may encompass large uncertainties since the method is limited by data and knowledge transfer gaps between
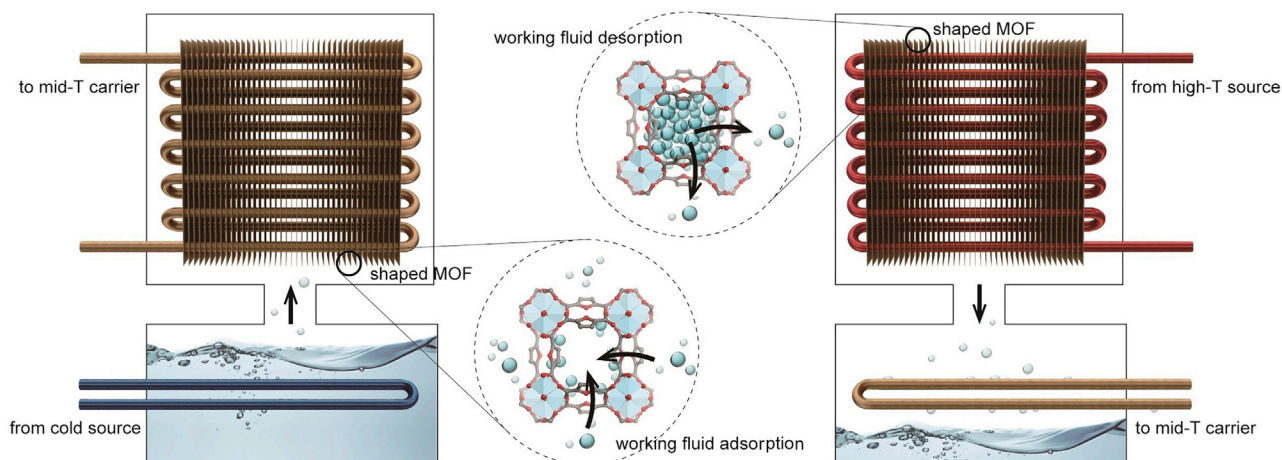
Figure 1. Schematic illustration of MIL-160(Al) based adsorption chiller

A MOF chiller comprises at least 2 identical reactors, regenerator and adsorber, exchanging refrigerant (i.e., water vapor) with a condenser and an evaporator alternately. The complete cycle has 4 temperature stages controlled by external thermal carrier fluid, which is also water in this case. The enthalpy supplied by the heat source at a high temperature to the reactor containing MOF with higher water uptake induces desorption of vapor at the condenser pressure. This vapor is liquefied in the condenser at an intermediate temperature and the MOF is dried to a lower water uptake, equilibrium state at the pressure. The reactor is then cooled down to an intermediate temperature and can adsorb vapor again. This vapor is produced by evaporating liquid refrigerant. Vaporization absorbs enthalpy from the heat source at a low temperature, creating a cooling effect. For convenience, the 2 intermediate temperatures are equal to ambient temperature.

disciplines. In addition to the materials-level innovation and validation, efforts are urgently needed to prove the fully functional system performance and to demonstrate its scalability if this alternative technology is poised to receive the market's attention and institutional incentives, similar to other emerging renewable energy branches in their early stage.

In this study, we conducted a complete investigation of state-of-the-art aluminum-carboxylate MOFs in cooling applications with various experimental techniques, examining how their major physical properties influence the macroscopic energy and power performance. A full-scale sorption chiller based on Al-MOFs is fabricated in this work (Figure 1). The COPs and SCPs are derived from thorough measurements on the refrigerant flow and the thermal carrier flow passing through two adsorbers, one condenser and one evaporator that operate continuously. Comparative tests reveal that selected MOFs exhibit an SCP surpassing 1 kW/kg, a 3-fold increase compared to silica gel, while within the same harsh operation ranges as the commercial absorption chiller based on LiBr. It is noteworthy that all MOFs are fabricated in-house under sustainable synthesis conditions, to address the requirements of industrial processes (e.g., reflux synthesis, non-toxic reactants, green solvents). We also compare our results with the commercial benchmark technology, compression chiller, under the same weather conditions.

Our work presents a key demonstration to future studies amid chemistry and energy engineering. We verify the effectiveness and shortages of analysis and characterization methods at different scales. Furthermore, while the MOF chiller is attaining unprecedented energy and power performance compared to existing sorption technology, its energy conversion efficiency still falls far behind the mainstream electricity-driven chiller. However, it is worth noting that the diurnal performance of a solar heat-powered MOF chiller (solar-to-heat-to-cooling) is comparable to that of a photovoltaic (PV) solar-driven compression chiller (solar-to-electricity-to-cooling) in terms of time-averaged COP, as discussed further in the article. To

reinforce the role of the thermally driven chiller in the climate mitigation plan, the economic viability of the technology must be approved. The methodology and results from this work lay the foundation regarding precise bottom-up techno-economic analyses for the next step.

RESULTS

Scalable preparation of Al-MOFs and shaping

A MOF chiller is a closed heat reallocation system only exchanging enthalpy but not mass with the environment, although the refrigerant and thermal transfer carrier here are both water (Figure 1). Each operation unit of the chiller is composed of two heat exchangers connected to each other: one contains MOF as the adsorbent, and the other one stocks refrigerant liquid. As long as the MOF has not attained the thermodynamic equilibrium state, which is determined by its isotherm curve under a given temperature and pressure, there is an adsorption potential to continuously draw the refrigerant vapor from the reservoir to the adsorption bed. It is preferred that the unit maintains a vapor-saturated pressure so that refrigerant boils off vigorously. Therefore, the lower the relative pressure where the inflection point of the isotherm is situated, the lower the evaporation temperature the reservoir can achieve. Once reaching equilibrium loading, the MOF drives no more vapor mass transport, and the cooling effect stops. MOF needs to be heated to evacuate the adsorbed vapor for use in the next cycle. We show the thermodynamic cycle in Figure S1 for 2 typical cooling applications of air conditioning (evaporating temperature T_{ev} = 10°C) and district cooling (T_{ev} = 20°C) in a summer condition (ambient temperature T_{amb} = 30°C). Briefly, the entire loop combined multiple mass and heat transport mechanisms, including bulk vapor movement between heat exchangers, diffusion within the adsorbent layer and MOF particles, heat transfer alongside vapor transport, and conduction between MOF, heat exchanger, and thermal carrier flow. Since the COP of the sorption cycle is calculated as delivered cooling energy amount divided by the energy input to regenerate the MOF, all other parasitic heat losses or transport impediments appearing in each step are undesirable.

As a result, a way to obtain a high COP and effective energy conversion, from thermodynamic perspectives, bypassing the barriers imposed on mesoporous solids, is to use hydrophilic microporous MOFs. These sorbents should possess higher uptakes at lower relative pressure while being regenerated at a low temperature to avoid sensible heat loss and enable low-grade energy source uses. State-of-the-art microporous Al-carboxylate MOFs show satisfactory results on both thermodynamic advantages and cyclic stability, with some prominent examples being MIL-160 (Al-FDC; FDC, 2,5-furandicarboxylate),[33] KMF-1 (Al-PyDC; PyDC, 2,5-pyrroledicarboxylate) (KMF: KRICT-CNRS-Montpellier Framework),[34] CAU-10 (Al-BDC; BDC, isophthalate) (CAU: Christian-Albrechts-Universität),[21] MIL-53-TDC/CAU-23 (Al-TDC; TDC, 2,5-thiophenedicarboxylate),[35] MOF-303 (Al-PZDC; PZDC, 3,5-pyrazoledicarboxylate),[36] and MIL-53-Fum (Al-Fum; Fum, fumarate).[20,37]

Recent progress in scalable and green synthesis of MOFs has raised the conventional wisdom that their industrialization in the thermal energy area is unattainable due to the high production costs.[38–40] The present work contributes to this endeavor by improving the large-scale fabrication of several MOFs composed of Al, an abundant metal source, and widely available carboxylic organic linkers in commodity markets. Precisely four microporous Al carboxylate MOFs, MIL-160, Al-Fum, CAU-10, and CAU-23, were synthesized and shaped for the cooling application, with various hydrophilicity that their inflection points covered 0.08–0.28 p/p_0 (Figure S2).

Table 1. Main properties of tested MOFs for the application of adsorption chiller

Materials	Formula	Crystal density (g · cm^{-3})	Pore volume (cm^3 · g^{-1})	BET surface (m^2 · g^{-1})	Water uptake (g · g^{-1} dry mass)[a] Vapor pressure (p/p_0)				Energy density (Wh · kg^{-1})[b] Regeneration temperature (°C)			
					0.1	0.2	0.3	0.4	60	70	80	90
MIL-160[33]	Al(OH)(C$_6$H$_2$O$_5$)	1.09	0.4	1,070	0.223	0.34	0.356	0.362	40	91	185	262
CAU-10[40]	Al(OH)(C$_8$H$_4$O$_4$)	1.15	0.25	656	0.003	0.224	0.231	0.246	29	188	193	196
CAU-23[35]	Al(OH)(C$_6$H$_2$O$_4$S)	1.07	0.48	1,250	0.002	0.025	0.32	0.351	226	254	256	259
Al-Fum[20]	Al(OH)(C$_4$H$_2$O$_4$)	1.06	0.47	1,025	0.024	0.046	0.325	0.372	211	261	269	275
Silica gel	SiO$_2$	1.35	0.44	760	0.031	0.056	0.091	0.113	47	58	65	72

[a]The change of isotherms is limited at different temperatures (see Figure S3).
[b]Cyclic operation at T_{ev} = 15°C and T_{ad} = 30°C. The enthalpy of water condensation is taken at T_{cd} = 30°C.

The MOF syntheses were adapted for scale-up purposes toward industry-orienting processes, improving the overall total space-time-yield (STY) of the product (i.e., STY taking into accounts washing procedures). For instance, we have notably shortened the total preparation time for MIL-160 to adapt to mass production. The synthesis of MIL-160 was performed in a 30-L kilo lab reactor with mechanical stirring. A mixture of Al acetate, basic, and 2,5-furandicarboxylic acid was vigorously stirred in deionized water under reflux conditions. After the one-step reaction, a white product was collected by filtration. A 25L Nutsche filter in which the washing of the product took place directly was used precluding additional long steps with successive filtration, recovering, and washing cycles. The overall time is thus greatly reduced, thereby lowering the overall total STY. The production yield was 93% and the synthesis STY was 185 kg · m^{-3} · day^{-1}. The product quality was confirmed and compared with previously reported values obtained from small-scale synthesis[33,41] by powder X-ray diffraction (PXRD), nitrogen adsorption test, and thermogravimetric analysis. The green process and high yields are the key factors for industrialization (Figures S4–S7). Details of syntheses of other MOFs are found in the supplemental experimental procedures. We list the key parameters of synthesized Al-MOFs for use in the adsorption chiller in Table 1, in comparison to a conventional adsorbent silica gel. The cyclic water uptake at different vapor pressure and cooling energy density at different regeneration temperatures determine the optimum operation conditions of each MOF in an adsorption chiller. All MOFs demonstrate here a step change at the inflection points compared to the linear change in silica gel.

A simple and scalable coating process was also used to deposit the MOF powders on the heat exchanger. The selected powders were dispersed in deionized water. A binder of organic silicone was added to the suspensions under continuous stirring to provide stable coatings. At first, the coating process was performed manually and on a small scale for the needs of kinetic tests, and then a dip-coating process was used for the full-scale heat exchangers. The coated samples were dried and cured at 150°C to obtain the optimal mechanical strength. No evident peeling of the coating layers was observed after all of the tests.

Characterization, modeling, and design of MOF heat exchangers

From the point of view of kinetics, it is essential to characterize the power performance of a representative MOF heat exchanger (HEx) rather than the pristine MOF materials, capturing pertinent heat and mass transport constraints. A large temperature jump" (LTJ) method is generally considered in the thermal engineering community to simulate the working cycles of an adsorption chiller at a reduced scale to make a low-cost and fast evaluation.[27,42] We adopted a gravimetric LTJ method
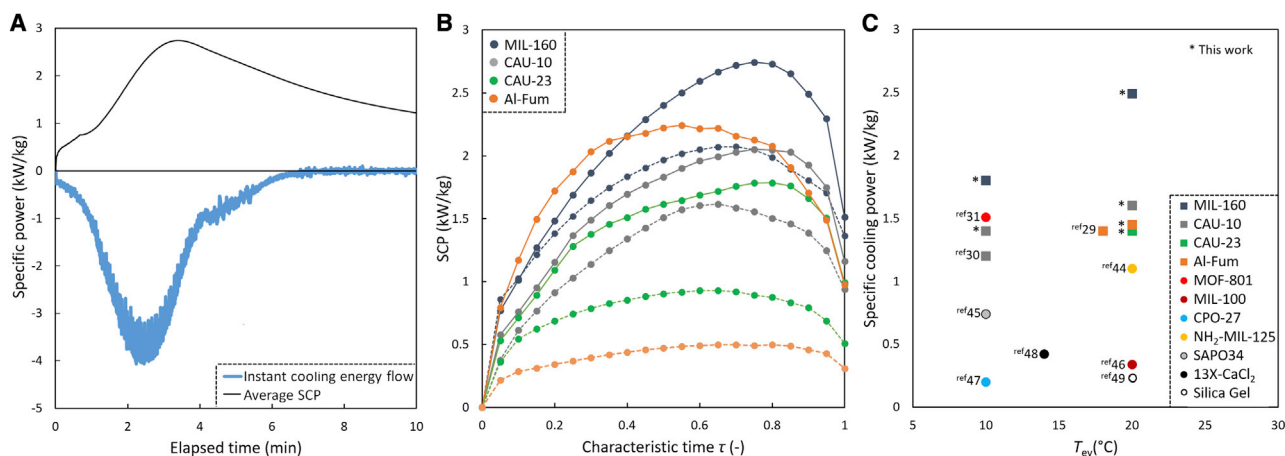
Figure 2. Al-MOFs water sorption dynamic performance obtained from small-scale test
(A) Instant cooling flow rates and average SCP of the evaporator connected to a MIL-160 adsorber.
(B) Average SCP over different characteristic adsorption time with Al-MOFs at T_{ad} = 30°C, and T_{ev} = 20°C (unbroken lines), or 10°C (broken lines).
(C) Comparison of cooling power of Al-MOFs/water pairs adsorption chiller with benchmark sorbents. Values are presented with configurations of 0.4–0.5 mm coating (square marks) or 0.8–1 mm granules (circle marks).
Data from Solovyeva et al.,[31,44] and Girnikab and Aristov[45] are based on monolayer samples with direct contact to the metal support; the impact of heat resistance is therefore less significant at low adsorption temperature and the configuration is to some extent comparable to the coating configuration. Data from AL-Dadah et al.,[46] Youssef et al.,[47] Chan et al.,[48] and Graf et al.[49] are based on fully packed columns in which the thermal resistance is much higher.

by positioning a small piece of Al sheet coated with Al-MOF layer under pure-vapor environments (with N_2 pressure <200 Pa for valve compensation), weighing it in continue, and varying the sample temperature in accordance with temperature triples for adsorption chiller (Figure S8; Note S1). The adsorption kinetic characteristics as well as the SCP were deduced from the temporal evolution of MOF HEx mass in a pressure-temperature-swing operation. We show a mass change profile example of a MOF HEx based on MIL-160 and resulting instant thermal flow rate in Figure S9. Figure 2A shows the instant cooling energy flow in the evaporator connected to the MOF HEx during adsorption (blue line). It is converted to average SCP (black line) at a given adsorption time. Note that the results manifest faster adsorption kinetics by 4–6 times more than a similar sample measured in the ambiance in a previous study,[43] which justifies the necessity of maintaining low-pressure operation conditions for adsorption chiller. A dataset is then collected on three other MOFs in Figure 2B. SCP is normalized in the function of average time to achieve equilibrium (τ) as a function of temperature (T) and partial pressure (p/p_0) in the two scenarios of air conditioning (T_{ev} = 10°C) and district cooling (T_{ev} = 20°C). These are also the most tested scenarios in the literature. For all MOFs, SCP drops when approaching equilibrium ($τ_{100\%}$) due to a loading-driven adsorption mechanism, which implies that a trade-off must exist between COP and SCP.

The measured SCP with benchmark adsorbent materials is mapped into Figure 2C, including various MOFs, silica gel, and zeolites identified from the literature.[29–31,44–49] The Al-MOFs series exhibit a marked mass power density that is 5 times higher than the conventional adsorbents, knowing that the cyclic water uptakes (energy density) are also 2–4 times higher, which is of interest for many volume-limited urban scenarios. A very hydrophilic MOF MIL-160 can maintain a fairly high cooling power even for a classic space air conditioning design temperature 7°C–12°C, allowing an equivalent operation range to the LiBr absorption chiller, which cannot be achieved by commercially available silica gel adsorption chillers.[15,50]

With a much higher heat flow throughput, it is challenging that a full-scale MOF HEx constantly operates under isothermal conditions, and the inappropriate design of MOF HEx can have an unfortunate impact on transient adsorption, especially when the low heat conductivity of the porous structure of MOFs is taken into account.[51] The advantage of the steep S-shape isotherms of MOFs can convert to shortages if the adsorbers are not meticulously engineered. For instance, a slight temperature shift will result in a large water uptake move when the vapor pressure is close to the inflection points, which would deteriorate the power output and hence the COP.

To determine a set of optimal design parameters for the manufacture of full-scale adsorbers, we adopted a protocol based on experience, simulation, and technical possibilities.[52] We studied three key design parameters of the MOF HEx—the adsorbent thickness, the fin thickness, and the fin space—which turned out to be influential in energy efficiency. Because the cyclic operation switches between reversible adsorption and desorption, the sorption enthalpies of which are almost equal, the energy loss mainly originates from sensible heat consumption. The sensitivity of COP to the MOF HEx geometry was monitored using the temperature triples from kinetic tests (Note S2). Principally, in typical MOF HEx configurations, adding more adsorbent reduces sensible heat loss while increasing thermal resistance. Reducing the coating layer thickness or particle porosity decreases vapor diffusion resistance but requires more frequent cycling, hence more irreversible thermal loss.

Although MIL-160 can thermodynamically achieve a cooling COP near 0.8 with these temperature profiles, the marginal effect on energy efficiency drops quickly by increasing sorbent layer upon 0.3 mm, and probably also the SCP, which evolves in inverse proportion to the COP. From a system perspective, at least two adsorption units functioning in alternate modes are necessary for continuous cooling production, and there is thus a need to balance the adsorption and desorption phase time between mode switches. As a trade-off, we chose a sorbent layer of 0.4 mm, fin thickness, and spacing of 0.3 and 1.5 mm for the following analysis and fabricating the full-scale prototype (Figures S10–S13).

Energy performance of Al-MOF HEx in a full-scale adsorption chiller

With the optimal choices of geometry and materials, we carried out a full-scale validation to prove the energy and power performance of the MOF chiller. Different MOF HExs based on MIL-160, CAU-10, and Al-Fum were in parallel coated. A uniform fin-tube HEx weighted 2.7 kg (coated part 490 × 183 × 110 mm) was used, with die-casting aluminum fins (0.3 mm) on copper tubes (ϕ11.9 mm) (Figure 3A). The MOFs were dip-coated twice with an organic silicone binder to achieve the ideal thickness.[53,54] Note that during the drying step, the gravity made the coating more challenging than in the case of the small-scale samples, resulting in less homogeneous layers, and each HEx was slightly different in weight.

A single-effect continuous adsorption chiller was fabricated and was composed of two adsorbers (finned-tube MOF HEx), an evaporator and a condenser (plate HEx) (Figure 3B). The components were assembled, with the vapor side connected and controlled with electromagnetic valves and the water side connected to a thermal bath, allowing a secondary thermal carrier fluid circuit to regulate the temperatures (Note S3). Finally, thermal and pressure meters at various positions were implemented to record the system states. A detailed schema of the instrumentation is presented in Figure S14.
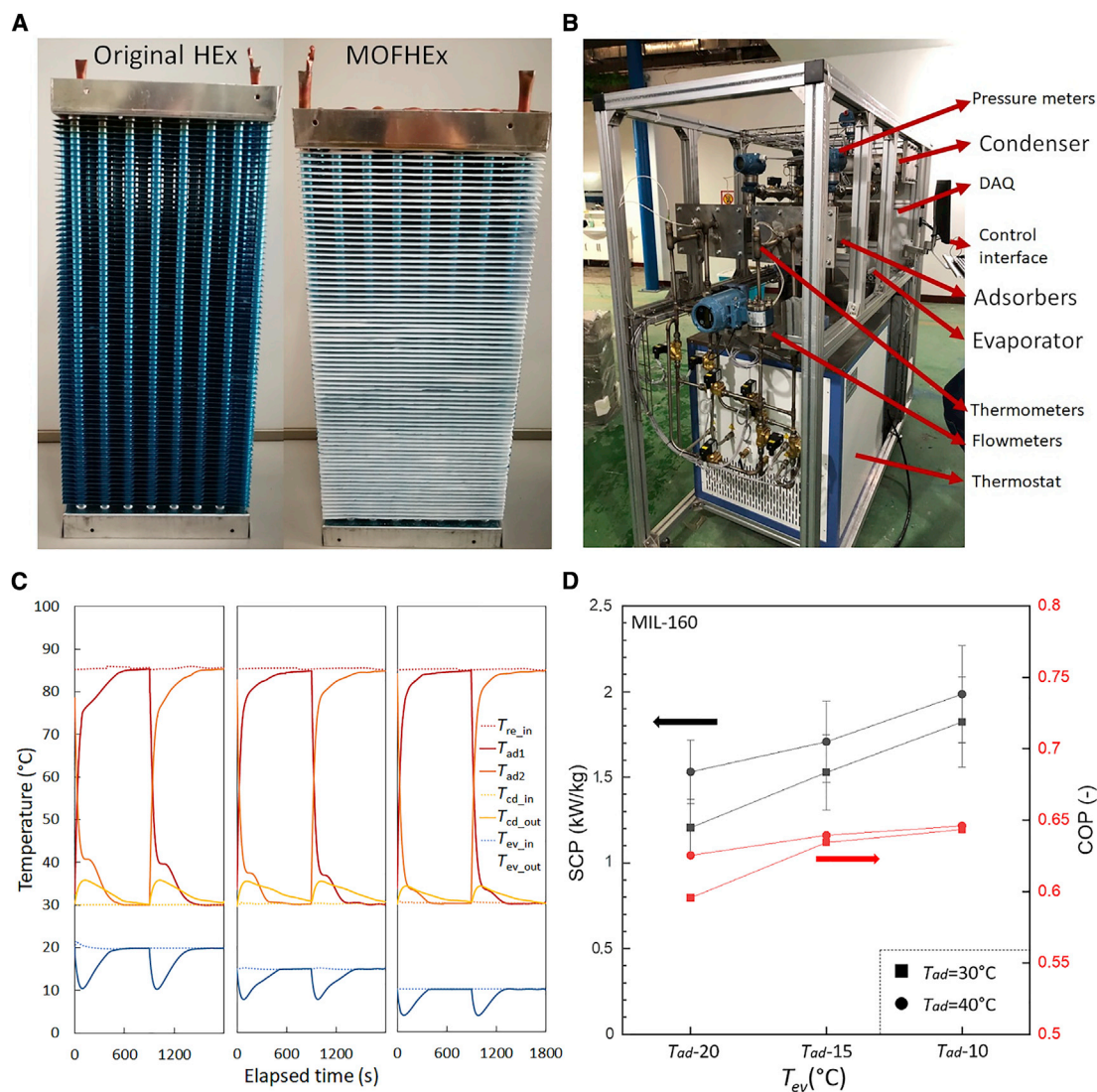
Figure 3. Test of full-scale adsorption chiller based on Al-MOFs

(A) Photograph of MOF HEx coated with MIL-160.

(B) Photograph of the test platform. All of the components, including containers and tubes, were thermally insulated before experiments.

(C) Temperature profiles of heat carrier at different components of the MIL-160 chiller. Broken lines represent flow inlet; unbroken lines represent flow outlet. The evaporator was connected to a low-temperature source, and T_{ev} inlet varied from 20°C and 15°C to 10°C. The condenser was connected to a medium-temperature source. The adsorbers switched between the medium- and high-temperature sources so that the T_{cd}/T_{ad} inlet was fixed at 30°C and the T_{re} inlet was fixed at 85°C.

(D) Measured SCP and COP at $\tau_{100\%}$ for MIL-160 by varying T_{ad}/T_{re} = 30°C/85°C and 40°C/95°C, with T_{ev} lower than T_{ad} by 10°C, 15°C, and 20°C. Error bars represent measure uncertainty from the flowmeters, thermometers, and layer thickness.

Figure 3C shows the temperature profile of the heat carrier fluids at variable T_{ev} (inlet temperature 10°C/15°C/20°C) with fixed T_{ad} (inlet temperature 30°C) and T_{re} (inlet temperature 85°C). The coated adsorbent mass with MIL-160(Al) was 844 and 860 g for the 2 adsorbers, and the coating layer thickness was 445 ± 95 μm. The average adsorption time was 356, 495, and 454 s. The pressure record inside each component verified the sorption cycling process (Figure S15). At the beginning of the adsorption half-cycle, the vapor side of the adsorber was isolated from the evaporator and its fluid side was connected to the recooling circuit. The pressure in the adsorber decreased quickly from a higher level in the previous desorption phase

during this isosteric cooling phase. The valve between the adsorber and the evaporator was open when the pressures were balanced. The pressure in the adsorber continued to drop below the evaporating pressure at T_{ev}, which attracted the movement of refrigerant vapor from the evaporator to the adsorber. After the adsorbent was saturated, the vapor pressure between the adsorber and the evaporator became equal again and the adsorption half-cycle was considered finished. Then, the adsorber was connected to the hot water circuit and he valve to the condenser was switched on after an isosteric heating phase. The pressure increased quickly to a higher level, which drove the released refrigerant vapor from the adsorber to the condenser, until the desorption half-cycle was complete.

The heat extracted by the evaporator or supplied to the adsorber was the product of the specific heat capacity of water, the outlet and inlet temperature differences, and flow rates of the thermal carrier fluids. The SCP is calculated as the extracted heat on the evaporator divided by the adsorption phase time, and the COP is the ratio of the produced cold and supplied heat (experimental procedures). At T_{ev} = 10°C, the saturated vapor pressure is equal to 0.3 p/p_0 at T_{ev} = 30°C, which is close to the inflection point, and the absolute pressure is very low; thus, both water uptake and adsorption kinetics were limited. The adsorption time at 20°C (0.55 p/p_0) is shorter than at 15°C (0.4 p/p_0), mostly due to higher pressure since the water uptakes at equilibrium had few distinctions. Figure 3D shows the energy performance results of MIL-160 that the COP at different T_{ad} kept almost the same, except for T_{ev} = 10°C, where the heat transfer efficiency was low. This tendency remained consistent for both CAU-10 and Al-Fum, as long as we held the temperature difference between T_{ad} and T_{re} (Figure S16).

The positions of the inflection points have a decisive impact on the regeneration temperature. In practice, we often set T_{ad} and T_{cd} as the ambient temperature; the regeneration temperature must be higher for ~45°C, ~40°C, and ~35°C, respectively, for MIL-160, CAU-10, and Al-Fum to achieve sufficiently high efficiency.

MOF adsorption chiller as a resilient solution to adapt to weather fluctuation

Solar heat-driven cold production using sorption-based chillers is a promising solution to shift away from the consumption of finite fossil fuel resources. In this section, the results of a semi-field test carried out in representative outdoor conditions are presented. The time-resolved diurnal thermodynamic performance of the MIL-160 MOF adsorption chiller coupled to an array of evacuated-tube collectors (ETCs) is predicted during a hot sunny day (July 2020, Paris), which exhibits significant solar irradiance and ambient temperature fluctuations. The instantaneous cooling power is measured from the full-scale MIL-160 prototype, while the ETC efficiency is determined as a function of the incident solar flow and ambient and hot water temperatures (Note S3).

Heat is rejected to the outdoor air in the adsorber and condenser units, respectively, at T_{ad} and T_{cd}—both assumed equal to the instantaneous ambient temperature, T_{amb}, while the cooling effect is produced within the evaporator unit, maintained at T_{ev} = 10°C. The adsorption chiller is operated so as to maintain a regeneration temperature, T_{re}, 50°C above the ambient temperature. The chiller is operated from 10:00 to 18:00 (i.e., 10 a.m.–6 p.m.), with an adsorption phase time of 600 s. The collected and processed time-resolved data are reported in Figure 4, from which one can observe that the ambient temperature slowly ramps up from 20°C to 30°C between 9:30 and 12:30 and drops from 17:00 onward, while the incoming solar irradiance fluctuates around a mean value of 800 W/m^2.
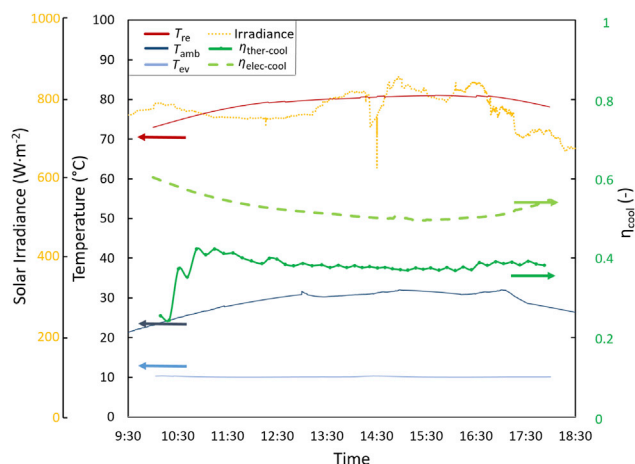
Figure 4. Roadmap comparison between solar-to-heat-to-cooling and solar-to-electricity-to-cooling

$\eta_{\text{ther-cool}}$ is the global conversion efficiency from solar radiation to a thermally driven MIL-160 adsorption cooling system measured from outdoor test (details in Figure S18). $\eta_{\text{elec-cool}}$ is simulated global conversion efficiency of a compounded system on photovoltaics and compression-based chiller. Evaporating and condensing temperatures of both systems are set to be ambience temperature and 10°C, respectively.

The instantaneous thermodynamic performance of the chiller in said operating conditions is monitored through the COP and SCP of each adsorption cycle, similar to the analysis performed in the controlled laboratory environment. In addition, the overall solar-to-cooling conversion efficiency, $\eta_{\text{ther-cool}}$, is obtained as the product of the thermal efficiency of the solar ETC system, η_{th}, and the COP of the adsorption system:

$$\eta_{\text{ther-cool}} = \eta_{\text{th}} COP \qquad \text{(Equation 1)}$$

where $\eta_{\text{ther-cool}}$ is the ratio of the useful cooling power to the incident solar irradiance, the instantaneous value of which, shown in Figure 4, stabilizes at ~0.4 from the third adsorption cycle.

To further appreciate the daily performance of this adsorption-based system, its efficiency is compared to that of a typical, commercially available competing technology. The overall solar-to-cooling efficiency of an electrically driven vapor-compression chiller combined with an array of PV solar panels is predicted for the same ambient and solar irradiation history, whereby the dependence of the efficiency of the PV panels upon their temperature is accounted for, while the vapor-compression cycle COP is derived from manufacturer performance maps (Figure S19) as a function of the evaporation and condensation temperatures, which are assumed to equal the heat removal (cooling) and heat rejection (ambient) temperatures, respectively.

Whereas the solar-to-cooling conversion efficiency of the solar-heat-driven MOF chiller, which takes values ~0.4 ($\pm$0.05), is lower than that of the PV-driven vapor compression chiller, which takes values ranging between 0.5 and 0.6, it exhibits smaller fluctuations during the day. This reflects the greater dependence of the compression-based system performance upon the time-varying operating conditions compared to the adsorption system, which is due to the large variation of the electrical efficiency of the PV panels and of the COP of the mechanical compressor in the former with the varying conditions. The MOF chiller does not

exhibit these strong variations, as the efficiency of the solar thermal generation system is less sensitive to the ambient temperature and irradiance, and variations to the COP are alleviated if the system vapor pressure is retained at the right side of the inflection point. Note that the comparison between the two roadmaps is merely from an engineering perspective with no thermodynamic meaning because the temperature stages and energy grades of the cycles are all different.

Therefore, although they may not have better steady-state performance than compression-based cooling systems available on the market, and although they are more bulky, solar-cooling systems based on MOF chillers may find application opportunities in scenarios with high renewable penetration to the grid where electrification presents greater challenges, as well as in off-grid or areas with poor or intermittent electricity supply, where storage is required to keep the system operating. This is the case because electricity storage is more difficult and expensive than thermal storage. Furthermore, district cooling applications as well as applications in which industrial waste heat (or cold) or other renewable (e.g., geothermal, biomass) thermal resources are available are highly suitable for integration with MOF chillers, while additional advantages are offered by their silent and low-vibration operation, long lifetimes, and low maintenance requirements and costs. Of particular interest in recent years is the cooling of data centers, which are an especially suitable application for the implementation of MOF chillers.

DISCUSSION

An updated development strategy of adsorption cooling technology from de Lange et al.[15] and Schnabel et al.,[52] based on MOFs, or more generally on advanced adsorbents, can be summarized as follows:

(1) Stability: when water is the adsorbate, the essential data must come from the cyclic hydrothermal stability test. There is an ambiguity of the term *stability* in the literature. Many early studies claimed a new MOF as "water stable" by maintaining function after 5 or 10 adsorption cycles or immersing the MOF in water for a long duration. This is insufficient given that the operation of MOF water adsorption shall attain dozens of cycles per day. More risks are likely to occur in the breath-in and -out cycles of the adsorbates, which tend to destroy the crystalline structure of the MOFs.[55] For the practical application of MOF adsorption technology, stability information should be collected from hundreds or even thousands of cycles to allow a reliable estimate of the yearly degradation rates.

(2) Thermodynamic properties (i.e., the shape of isotherms, existence of hysteresis loop, enthalpy of adsorption), the combination of which can roughly calculate COP under given working conditions. MOFs are distinguished from conventional sorbents by the S-shape adsorption isotherms. In a recent review, Liu and coworkers[56] refined the criteria to find appropriate MOFs in thermal energy reallocation.

(3) Scale-up and green synthesis: the costs of MOFs can be divided into raw materials and production process. Usually, the larger the STY, the more economically viable the process. Still, the translation of STY obtained from small-scale synthesis to the industrial level is not straightforward. The calculation must be meticulously presented by considering the holistic production with washing/purification, activation, and drying. Although we focus on selected Al-based materials in this work, more MOF types are potentially suitable if scaling-up is realized.[57]

(4) Kinetics of shaped materials: the effective heat and mass transport characteristics should be measured at the macroscopic level to assess the system dynamics. As COP determines the consumption of source energy and operational costs and SCP determines the equipment size and initial investment, a thorough estimate of the levelized cost of thermal energy require both pieces of information.

(5) Full-scale validation in operational environments.

(6) Implementation under real conditions and various scenarios.

(7) Large-scale deployment: the seven stages from fundamental research to higher technology readiness levels can be consecutively developed, but they can also be forethoughtful studies with synergy between different disciplines. For instance, the actual market capacity of chillers or heat pumps contains adsorbents on the order of thousands of tons per annum; thus, designing novel MOFs to improve energy efficiency or power performance with valuable metals and expensive linkers is not a prioritized strategy. Another example is that advances in computational techniques and data science enable the performance prediction[58] before actually synthesizing the materials, and with precisely and robustly defined thermal engineering boundaries, the screening of structures can be quickly narrowed down to a smaller scope.

Unlike previous studies that concentrated mostly on material functionalities, we consider both the effects of material intrinsic properties and shaping configurations on the energy performance. For most water-stable MOFs, the isotherms maintain the same forms, sizes, and positions of adsorbed vapor in regard to relative pressure, despite a slight rightward shifting of the sorption step often observed at higher temperatures due to the increased free energy of the sorbate. The latter behavior benefits the usual operation cycle in an adsorption chiller with low-temperature adsorption and high-temperature desorption.

The contradiction in fulfilling both requirements on large temperature lift and low temperature regeneration must find compromised solutions. Our study shows clearly that hydrophilic adsorbents (MIL-160, CAU-10) can ensure low-temperature cooling energy flux for routinely designed air conditioner temperature windows of $7°C–12°C$. The energy efficiency can be maintained as long as the system pressure is situated at the right side of the sorption steps (MIL-160: >0.2 p/p_0; CAU-10: >0.25 p/p_0; CAU-23 and Al-Fum: >0.3 p/p_0). A higher pressure can improve the sorption kinetics to some extent, but it largely shrinks the achievable temperature lift.

Inflection points at even higher pressures are not practical for heat exchange between mechanical components of the adsorption chiller. For instance, the adsorbents MIL-100 (0.35 p/p_0) and MIL-101 (0.4 p/p_0) can only provide a temperature lift of $\leq 12°C$, despite that their water uptake can reach 0.6 and 1.6 g/g dry mass, respectively. However, very hydrophilic adsorbents, the inflection point of which is <0.05 p/p_0, can achieve a temperature lift of $\geq 40°C$ and are more adapted to scorching weather. Even though MOFs with such isotherms can dramatically lower the desorption temperature compared to X-type and Y-type zeolites,[59] the corresponding adsorption chiller is unsuitable for basic configurations with hot water circuits. In contrast, a combination of multiple-effect chillers with engine waste heat, concentrated solar thermal, and long-distance heating pipe is foreseeable.

We have confirmed that kinetic measurements at a small but macroscopic scale can hand over a relatively accurate estimate of energy performance. Our full-scale chiller with various Al-MOFs has a lower cooling power by 20% compared to the performances obtained from the small-scale kinetic tests on average. The vapor stayed in closed containers in the full-scale device in comparison to moving to an open terminal in the kinetic tests, which results in a slower mass transport, decreasing the generated power. The valves and adjacent pipes between components may have contributed to the pressure loss as well, leading to a reduction in the driving temperature difference and a loss of power. The energy efficiency is also slightly lower. Besides the sensible loss taken into account in the kinetic tests, there is more irreversible energy loss in the full-scale device responsible for this discrepancy, including the sensible transfer loss of the liquid water between the condenser and the evaporator and the transport loss of overheating during the phase change of the refrigerant. The latter can be estimated from the exergy consumption of the system, as shown in Figure S17. In short, since the volumetric energy density of MOF HEx is much higher than conventional adsorbents, the cyclic adsorption and desorption generate larger vapor flux, which more easily induces overpressurized or overheating environments for the operation and increases irreversible losses. The transport efficiency can be enhanced by raising the water-side flow and tube sizes, reducing the dead volume of the containers, and controlling the vapor flow with more intelligent operation strategy of the valves. It can be expected that a device with a common commercialized size >50 kW can largely remove the irreversible losses compared to the demonstration in this article.

All of the above principles determining the overall performance of an adsorption chiller also work for space heating applications. The thermodynamic and kinetic properties of MOFs do not vary significantly in the temperature ranges. It is worth noting that the global heating needs, unlike the boosted cooling needs, will remain relatively steady in future decades.[5] Because most of the heating needs are satisfied by fossil fuels at present,[60] the market requires structural reform as per climate mitigation plans. An all-embracing electrification strategy, currently being put forward by many, may, however, increase the vulnerability of today's heating system when exposed to extreme circumstances, given that an electric heat pump alone holds less resilience capacity.[61] Promoting renewables and building retrofits will be favorable to MOF adsorption devices using a comparable low-cost solar ETC in either a distributed or centralized scenario for source, as the whole system has zero marginal costs. A MOF heat pump harnesses thermal energy from a low-temperature surrounding to a middle-temperature heat sink. The heating COP equals the cooling COP plus one since it amplifies the energy quantities by degrading the heat inputs from the high-temperature source. The tested hydrophilic Al-MOFs can maintain high performance in temperate climates, where the soil temperature for design in winter is ~10°C (e.g., France, the UK, the Netherlands), and the temperature lifts can be sufficient in more volatile situations with well-insulated buildings.[62]

Admittedly, space heating in colder climates or for high-energy-loss buildings shall search for larger temperature lifts. More hydrophilic MOFs may not demonstrate better performance since water has its limitations in evaporating temperature. An alternative is to change the sorbate to small alcohols, which can extend the cooling temperature below 0°C.[63] The development stage of MOFs/alcohols are less mature since characterization and screening still need to be accomplished beyond a handful of archetypal materials.[64,65] The stronger affinity to alcohols compared to water often indicates a different type of isotherm (Y-shape instead of S-shape)—

thus a higher regeneration temperature and a higher risk of destroying the crystalline structure in cyclic operations. In Nordic and arctic climates where solar radiation is less available, the second type of adsorption heat pump (i.e., adsorption heat transformer),[66] as another possible choice, can be applied to harvest heat from deep cold or for upgrading geothermal sources. The system rejects condensation heat to a lower temperature (air), driven by low pressure enabled by a frigid environment (below $-15°C$), and the adsorbate evaporates at a middle temperature for waste heat upgrading (building exhausts, soil, and sea). Solovyeva and coworkers[67] have provided experimental evidence of MIL-101/methanol for ambient heating in Russian winter, where the efficiency of electric heat pumps is low. The thermodynamic cycle of adsorption heat transformation has a lower COP than the regular adsorption heat pump in the same temperature triple. This is because the switch of adsorption and desorption temperature stages does not facilitate sorption step shifting. Even so, the system is worth investigating, since both low- and middle-temperature sources are freely accessible. The most sustainable energy is what we have wasted.

In summary, we highlight the advantages of water-stable microporous Al-carboxylate based MOFs (Al-MOFs) as sorbents in the application of adsorption cooling in this study. These Al-MOFs (i.e., MIL-160, CAU-10, Al-Fum, and CAU-23) have been synthesized along green and scalable processes, which are prerequisites for exploring various industrial and civil scenarios. Based on the optimal configuration, a full-scale adsorption chiller on Al-MOFs with different adsorption isotherms is designed to validate the production of cold from heat (and vice versa). The tested Al-MOFs all achieve COP above 0.6 and SCP over 1 kW/kg in typical working conditions. When solar thermal is used as the heat source for the adsorption chiller to produce cold, Al-MOFs provide weather-resilient solutions, with relatively stable COP outputs regarding environmental temperature fluctuation. Thus, the Al-MOF adsorption chiller has great potential to reduce abrupt heat exposure risks under the requirements of increasing renewable shares.

In comparing technology roadmaps for solar-to-cooling using a MIL-160 chiller and a commercially available vapor-compression air conditioner, the former demonstrates a lower efficiency by 30%. This inspires the future research strategy in heat-driven cooling. The levelized cost of cooling energy should be acceptable to compete with the latter via either lowering the costs of materials or improving the energy conversion efficiency at a system level in making good use of the advanced sorbents.

EXPERIMENTAL PROCEDURES

Resource availability

Lead contact
Further information and requests for the resources are available from the lead contact, Frédéric Cui (f.s.cui@tue.nl).

Materials availability
This study did not generate unique materials.

Data and code availability
Details about the synthesis of materials and the data used to draw the conclusions can be found in the experimental procedures and the supplemental information. Requests for further data will be fulfilled by the lead contact.

Methods for energy performance calculation

The energy efficiency is equal to the ratio of cooling energy produced over heat energy consumed:

$$COP = \frac{\int_0^{\tau_{ad}} dQ_{ev} dt}{\int_{\tau_{ad}}^{\tau_{de}} dQ_{de} dt}.$$ (Equation 2)

Calculation of COP in the kinetics tests and numeric simulation:

$$COP = \frac{\int_{w_{ad}}^{w_{re}} H_{ev}(water) dw}{\int_{T_{ad}}^{T_{re}} (m_{HEx} c_{p,HEx} + m_{ad} c_p) dT + \int_{w_{ad}}^{w_{re}} H_{ad} dw};$$ (Equation 3)

where $H_{ev}(water)$ is the water evaporation enthalpy at T_{ev}, H_{ad} is the adsorption enthalpy of the MOF at T_{re}, m_{ad} and m_{HEx} are the adsorbent and HEx mass, c_p and $c_{p,HEx}$ are the effective heat capacity of the adsorbent and HEx, w is water uptake. The heat properties were obtained according to Cui et al.[51]

The calculation of SCP in the kinetics tests and numeric simulation was as follows:

$$SCP = \frac{\int_0^{\tau_{ad}} dQ_{ev} dt}{m_{ad} \tau_{ad}}.$$ (Equation 4)

The calculation of COP with the full-scale adsorption chiller was as follows:

$$COP = \frac{\int_0^{\tau_{ad}} \dot{q}_{ev}(T_{ev,\,out} - T_{ev,\,in}) c_{p,water} dt}{\int_{\tau_{ad}}^{\tau_{re}} \dot{q}_{re}(T_{re,\,out} - T_{re,\,in}) c_{p,water} dt}.$$ (Equation 5)

where $\dot{q}$ is the flow rate of the thermal carrier circuits and $c_{p,water}$ is heat capacity of the thermal carrier water. The electricity consumption on valves and water pumps was <7% of the produced cooling energy and can be largely reduced when the chiller size increases; therefore, this was not considered in the analysis.

SUPPLEMENTAL INFORMATION

Supplemental information can be found online at https://doi.org/10.1016/j.xcrp.2021.100730.

AUTHOR CONTRIBUTIONS

Conceptualization, F.S.C. and C.S.; methodology, F.S.C., C.B., C.N.M., J.H., and C.S.; investigation, E.G., C.C., F.S.C., X.Z., P.S., and F.N.; writing – original draft, E.G., C.C., F.S.C. and P.S.; writing – review & editing, X.Z., F.N., C.B., C.N.M., J.H., and C.S.

DECLARATION OF INTERESTS

The authors declare no competing interests.

REFERENCES

1. Vautard, R., van Aalst, M., Boucher, O., Drouin, A., Haustein, K., Kreienkamp, F., et al. (2020). Human contribution to the record-breaking June and July 2019 heat waves in Western Europe. Environ. Res. Lett. *15*, 094077. https://doi.org/10.1088/1748-9326/aba3d4.

2. Christidis, N., Jones, G.S., and Stott, P. (2015). Dramatically increased chance of extremely hot summers since the 2003 European heatwave. Nat. Clim. Chang. *5*, 46–50.

3. Van Oldenborgh, G.J., Philip, S., Kew, S., Vautard, R., Boucher, O., Otto, F., Haustein, K., Soubeyroux, J.-M., Ribes, A., Robin, Y., et al. (2019). Human Contribution to the Record-Breaking June 2019 Heat Wave in France; World Weather Attribution (WWA).

4. Cui, S., Stabat, P., and Marchio, D. (2016). Numerical simulation of wind-driven natural ventilation: Effects of loggia and facade porosity on air change rate. Build. Environ. *106*, 131–142.

5. Santamouris, M. (2016). Cooling the buildings-past, present and future. Energy Build. *128*, 617–638.

6. Akbari, H., Cartalis, C., Kolokotsa, D., Muscio, A., Pisello, A.L., Rossi, F., Santamouris, M., Synnefa, A., Wong, N.H., and Zinzi, M. (2016). Local climate change and urban heat island mitigation techniques – the state of the art. J. Civ. Eng. Manag. *22*, 1–16.

7. Reese, A. (2018). Slow coolant phaseout could worsen warming. Science *359*, 1084.

8. IPCC (2015). Climate Change 2014: Mitigation of Climate Change. Contribution of Working Group III to the IPCC 5th Assessment Report. of the Intergovernmental Panel on Climate Change. O. Edenhofer, R. Pichs-Madruga, Y. Sokona, E. Farahani, S. Kadner, K. Seyboth, A. Adler, I. Baum, S. Brunner, P. Eickemeier, et al., eds. (Cambridge University Press).

9. IEA (2017). Energy Technology Perspectives 2017 (International Energy Agency).

10. Sarbu, I., and Sebarchievici, C. (2013). Review of solar refrigeration and cooling systems. Energy Build. *67*, 286–297.

11. Deng, J., Wang, R., and Han, G. (2011). A review of thermally activated cooling technologies for combined cooling, heating and power systems. Progr. Energy Combust. Sci. *37*, 172–203.

12. Meunier, F. (2013). Adsorption heat powered heat pumps. Appl. Therm. Eng. *61*, 830–836.

13. Moliner, M., Martínez, C., and Corma, A. (2015). Multipore zeolites: synthesis and catalytic applications. Angew. Chem. Int. Ed. Engl. *54*, 3560–3579.

14. Najjaran, A., Freeman, J., Ramos, A., and Markides, C.N. (2020). Experimental investigation of an ammonia-water-hydrogen diffusion absorption refrigerator. Appl. Energy *256*, 113899.

15. de Lange, M.F., Verouden, K.J.F.M., Vlugt, T.J.H., Gascon, J., and Kapteijn, F. (2015). Adsorption-driven heat pumps: the potential of metal–organic frameworks. Chem. Rev. *115*, 12205–12250.

16. Canivet, J., Fateeva, A., Guo, Y., Coasne, B., and Farrusseng, D. (2014). Water adsorption in MOFs: fundamentals and applications. Chem. Soc. Rev. *43*, 5594–5617.

17. Furukawa, H., Gándara, F., Zhang, Y.-B., Jiang, J., Queen, W.L., Hudson, M.R., and Yaghi, O.M. (2014). Water adsorption in porous metal-organic frameworks and related materials. J. Am. Chem. Soc. *136*, 4369–4381.

18. Maurin, G., Serre, C., Cooper, A., and Férey, G. (2017). The new age of MOFs and of their porous-related solids. Chem. Soc. Rev. *46*, 3104–3107.

19. Seo, Y.K., Yoon, J.W., Lee, J.S., Hwang, Y.K., Jun, C.-H., Chang, J.-S., Wuttke, S., Bazin, P., Vimont, A., Daturi, M., et al. (2012). Energy-efficient dehumidification over hierachically porous metal-organic frameworks as advanced water adsorbents. Adv. Mater. *24*, 806–810.

20. Jeremias, F., Fröhlich, D., Janiak, C., and Henninger, S.K. (2014). Advancement of sorption-based heat transformation by a metal coating of highly stable, hydrophilic aluminium fumarate MOF. RSC Advances *4*, 24073–24082.

21. Fröhlich, D., Pantatosaki, E., Kolokathis, P.D., Markey, K., Reinsch, H., Baumgartner, M., van der Veen, M.A., De Vos, D., Stock, N., Papadopoulos, G.K., et al. (2016). Water adsorption behaviour of CAU-10-H. A thorough investigation of its structure-property relationships. J. Mater. Chem. A Mater. Energy Sustain. *4*, 11859–11869.

22. Tschense, C.B.L., Reimer, N., Hsu, C.-W., Reinsch, H., Siegel, R., Chen, W.-J., Lin, C.-H., Cadiau, A., Serre, C., Senker, J., et al. (2017). New Group 13 MIL-53 Derivates based on 2,5-Thiophenedicarboxylic Acid. Z. Anorg. Allg. Chem. *643*, 1600–1608.

23. Sohail, M., Yun, Y.N., Lee, E., Kim, S.K., Cho, K., Kim, J.N., Kim, T.W., Moon, J.H., and Kim, H. (2017). Synthesis of highly crystalline NH2-MIL-125 (Ti) with S-shaped water isotherms for adsorption heat transformation. Cryst. Growth Des. *17*, 1208–1213.

24. Wang, S., Lee, J.S., Wahiduzzaman, M., Park, J., Muschi, M., Martineau-Corcos, C., Tissot, A., Cho, K.H., Marrot, J., Shepard, W., et al. (2018). A robust large-pore zirconium carboxylate metal-organic framework for energy-efficient water-sorption-driven refrigeration. Nat. Energy *3*, 985–993.

25. Yilmaz, G., Peh, S.B., Zhao, D., and Ho, G.W. (2019). Atomic- and molecular-level design of functional metal-organic frameworks (MOFs) and derivatives for energy and environmental applications. Adv. Sci. (Weinh.) *6*, 1901129.

26. Ehrenmann, J., Henninger, S.K., and Janiak, C. (2011). Water adsorption characteristics of MIL-101 for heat-transformation applications of MOFs. Eur. J. Inorg. Chem. 471–474.

27. Graf, S., Redder, F., Bau, U., de Lange, M., Kapteijn, F., and Bardow, A. (2019). Toward optimal Metal-Organic Frameworks for adsorption chillers: Insights from the scale-up of MIL-101(Cr) and NH2-MIL-125. Energy Technol. (Weinheim) *8*, 1900617.

28. Mouchaham, G., Cui, F.S., Nouar, F., Pimenta, V., Chang, J.-S., and Serre, C. (2020). Metal-organic frameworks and water: 'from old enemies to friends'? Trends Chem. *2*, 990–1003.

29. Kummer, H., Jeremias, F., Warlo, A., Füldner, G., Fröhlich, D., Janiak, C., Gläser, R., and Henninger, S.K. (2017). A functional full-scale heat exchanger coated with aluminum fumarate metal–organic framework for adsorption heat transformation. Ind. Eng. Chem. Res. *56*, 8393–8398.

30. Lenzen, D., Bendix, P., Reinsch, H., Fröhlich, D., Kummer, H., Möllers, M., Hügenell, P.P.C., Gläser, R., Henninger, S., and Stock, N. (2018). Scalable green synthesis and full-scale test of the metal–organic framework CAU-10-H for use in adsorption-driven chillers. Adv. Mater. *30*, 1705869.

31. Solovyeva, M.V., Gordeeva, L.G., Krieger, T.A., and Aristov, Y.I. (2018). MOF-801 as a promising material for adsorption cooling: equilibrium conversion and management. Energy Convers. Manage. *174*, 356–363.

32. Farrusseng, D., Daniel, C., Hamill, C., Casaban, J., Didriksen, T., Blom, R., Velte, A., Fueldner, G., Gantenbein, P., Persdorf, P., et al. (2021). Adsorber heat exchanger using Al-fumarate beads for heat-pump applications - a transport study. Faraday Discuss. *225*, 384–402.

33. Cadiau, A., Lee, J.S., Damasceno Borges, D., Fabry, P., Devic, T., Wharmby, M.T., Martineau, C., Foucher, D., Taulelle, F., Jun, C.-H., et al. (2015). Design of hydrophilic metal organic framework water adsorbents for heat reallocation. Adv. Mater. *27*, 4775–4780.

34. Cho, K.H., Borges, D.D., Lee, U.-H., Lee, J.S., Yoon, J.W., Cho, S.J., Park, J., Lombardo, W., Moon, D., Sapienza, A., et al. (2020). Rational design of a robust aluminum metal-organic framework for multi-purpose water-sorption-driven heat allocations. Nat. Commun. *11*, 5112.

35. Lenzen, D., Zhao, J., Ernst, S.-J., Wahiduzzaman, M., Ken Inge, A., Fröhlich, D., Xu, H., Bart, H.-J., Janiak, C., Henninger, S., et al. (2019). A metal-organic framework for efficient water-based ultra-low-temperature-driven cooling. Nat. Commun. *10*, 3025.

36. Fathieh, F., Kalmutzki, M.J., Kapustin, E.A., Waller, P.J., Yang, J., and Yaghi, O.M. (2018). Practical water production from desert air. Sci. Adv. *4*, eaat3198.

37. Alvarez, E., Guillou, N., Martineau, C., Bueken, B., Van de Voorde, B., Le Guillouzer, C., Fabry, P., Nouar, F., Taulelle, F., de Vos, D., et al. (2015). The structure of the aluminum fumarate metal-organic framework A520. Angew. Chem. Int. Ed. Engl. *54*, 3664–3668.

38. Reinsch, H. (2016). "Green" Synthesis of Metal-Organic Frameworks. Eur. J. Inorg. Chem. *27*, 4290–4299.

39. Rubio-Martinez, M., Avci-Camur, C., Thornton, A.W., Imaz, I., Maspoch, D., and Hill, M.R. (2017). New synthetic routes towards MOF production at scale. Chem. Soc. Rev. *46*, 3453–3480.

40. Tannert, N., Jansen, C., Nießing, S., and Janiak, C. (2019). Robust synthesis routes and porosity of the Al-based metal-organic frameworks Al-fumarate, CAU-10-H and MIL-160. Dalton Trans. *48*, 2967–2976.

41. Permyakova, A., Skrylnyk, O., Courbon, E., Affram, M., Wang, S., Lee, U.-H., Valekar, A.H., Nouar, F., Mouchaham, G., Devic, T., et al. (2017). Synthesis optimization, shaping, and heat reallocation evaluation of the hydrophilic metal-organic framework MIL-160(Al). ChemSusChem *10*, 1419–1426.

42. Aristov, Y.I., Dawoud, B., Glaznev, I.S., and Elyas, A. (2008). A new methodology of studying the dynamics of water sorption/desorption under real operating conditions of adsorption heat pumps: experiment. Int. J. Heat Mass Transf. *51*, 4966–4972.

43. Gkaniatsou, E., Meng, B., Cui, F., Loonen, R., Nouar, F., Serre, C., and Hensen, J. (2021). Moisture-participating MOF thermal battery for heat reallocation between indoor environment and building-integrated photovoltaics. Nano Energy *87*, 106224.

44. Solovyeva, M.V., Aristov, Y.I., and Gordeeva, L.G. (2017). NH2-MIL-125 as promising adsorbent for adsorptive cooling: water adsorption dynamics. Appl. Therm. Eng. *116*, 541–548.

45. Girnikab, I.S., and Aristov, Y.I. (2016). Dynamic optimization of adsorptive chillers: the "AQSOA™-FAM-Z02-Water" working pair. Appl. Therm. Eng. *106*, 13–22.

46. AL-Dadah, R., Mahmoud, S., Elsayed, E., Youssef, P., and Al-Mousawi, F. (2019). Metal-organic framework materials for adsorption heat pumps. Energy *190*, 116356.

47. Youssef, P.G., Dakkama, H., Mahmoud, S.M., and AL-Dadah, R.K. (2017). Experimental investigation of adsorption water desalination/cooling system using CPO-27Ni MOF. Desalination *404*, 192–199.

48. Chan, K., Tso, C., Wu, C., and Chao, C.Y.H. (2018). Enhancing the performance of a zeolite 13X / CaCl 2 – water adsorption cooling system by improving adsorber design and operation sequence. Energy Build. *158*, 1368–1378.

49. Graf, S., Eibel, S., Lanzerath, F., and Bardow, A. (2020). Validated performance prediction of adsorption chillers: bridging the gap from gram-scale experiments to full-scale chillers. Energy Technol. (Weinheim) *8*, 1901130.

50. Wu, W., Wang, B., Shi, W., and Li, X. (2014). Absorption heating technologies: a review and perspective. Appl. Energy *130*, 51–71.

51. Cui, S., Marandi, A., Lebourleux, G., Thimon, M., Bourdon, M., Chen, C., Severino, M.I., Steggles, V., Nouar, F., and Serre, C. (2019). Heat properties of a hydrophilic carboxylate-based MOF for water adsorption applications. Appl. Therm. Eng. *161*, 114135.

52. Schnabel, L., Füldner, G., Velte, A., Laurenz, E., Bendix, P., Kummer, H., and Wittstadt, U. (2018). Innovative adsorbent heat exchangers: design and evaluation. In Innovative Heat Exchangers, H.-J. Bart and S. Scholl, eds. (Springer), pp. 363–394.

53. Bendix, P.B., Henninger, S.K., and Henning, H.-M. (2016). Temperature and mechanical stabilities and changes in porosity of silicone binder based zeolite coatings. Ind. Eng. Chem. Res. *55*, 4942–4947.

54. Cui, S., Qin, M., Marandi, A., Steggles, V., Wang, S., Feng, X., Nouar, F., and Serre, C. (2018). Metal-organic frameworks as advanced moisture sorbents for energy-efficient high temperature cooling. Sci. Rep. *8*, 15284.

55. Rieth, A.J., Wright, A.M., and Dincă, M. (2019). Kinetic stability of metal-organic frameworks for corrosive and coordinating gas capture. Nat. Rev. Mater. *4*, 708–725.

56. Liu, X., Wang, X., and Kapteijn, F. (2020). Water and metal–organic frameworks: from interaction toward utilization. Chem. Rev. *120*, 8303–8377.

57. Wang, S., and Serre, C. (2019). Toward green production of water-stable metal-organic frameworks based on high-valence metals with low toxicities. ACS Sustain. Chem. Eng. *7*, 11911–11927.

58. Jablonka, K.M., Ongari, D., Moosavi, S.M., and Smit, B. (2020). Big-data science in porous materials: materials genomics and machine learning. Chem. Rev. *120*, 8066–8129.

59. Cadiau, A., Belmabkhout, Y., Adil, K., Bhatt, P.M., Pillai, R.S., Shkurenko, A., Martineau-Corcos, C., Maurin, G., and Eddaoudi, M. (2017). Hydrolytically stable fluorinated metal-organic frameworks for energy-efficient dehydration. Science *356*, 731–735.

60. Tschopp, D., Tian, Z., Berberich, M., Fan, J., Perers, B., and Furbo, S. (2020). Large-scale solar thermal systems in leading countries: a review and comparative study of Denmark, China, Germany and Austria. Appl. Energy *270*, 114997.

61. Connolly, D., Lund, H., Mathiesen, B., Werner, S., Möller, B., Persson, U., Boermans, T., Trier, D., Østergaard, P., and Nielsen, S. (2014). Heat roadmap Europe: combining district heating with heat savings to decarbonise the EU energy system. Energy Policy *65*, 475–489.

62. Gadd, H., and Werner, S. (2013). Daily heat load variations in Swedish district heating systems. Appl. Energy *106*, 47–55.

63. de Lange, M.F., van Velzen, B.L., Ottevanger, C.P., Verouden, K.J.F.M., Lin, L.-C., Vlugt, T.J., Gascon, J., and Kapteijn, F. (2015). Metal-organic frameworks in adsorption-driven heat pumps: the potential of alcohols as working fluids. Langmuir *31*, 12783–12796.

64. Rezk, A., Al-Dadah, R., Mahmoud, S., and Elsayed, A. (2013). Investigation of ethanol/metal organic frameworks for low temperature adsorption cooling applications. Appl. Energy *112*, 1025–1031.

65. Kummer, H., Baumgartner, M., Hügenell, P., Fröhlich, D., Henninger, S.K., and Gläser, R. (2017). Thermally driven refrigeration by methanol adsorption on coatings of HKUST-1 and MIL-101 (Cr). Appl. Therm. Eng. *117*, 689–697.

66. Engelpracht, M., Gibelhaus, A., Seiler, J., Graf, S., Nasruddin, N., and Bardow, A. (2020). Upgrading Waste Heat from 90 to 110 Degrees C: The Potential of Adsorption Heat Transformation. Energy Technol. (Weinheim) *9*, 2000643.

67. Solovyeva, M.V., Gordeeva, L.G., and Aristov, Y.I. (2019). "MIL-101(Cr)–methanol" as working pair for adsorption heat transformation cycles: adsorbent shaping, adsorption equilibrium and dynamics. Energy Convers. Manage. *182*, 299–306.